

Mass transfer at the electrodes of the 'falling-film cell'

F. COEURET, J. LEGRAND*

CNRS, Ecole Nationale Supérieure de Chimie de Rennes, Avenue du Général Leclerc, 35000 Rennes-Beaulieu, France

Received 23 January 1984; revised 24 May 1984

In the 'falling-film cell' the electrolyte flows as a thin film in the channel between an inclined plane plate and a sheet of expanded metal which work as electrodes. The present work gives the mass transfer coefficients at both electrodes; the experimental variables are the electrolyte flow-rate, the angle of inclination of the channel and the interelectrode distance. The results allow three different flow regimes to be characterized. At low flow rates, there exists a particular regime where capillary effects are present; in this regime the mass transfer coefficient decreases with increasing flow rate, which is interesting from the point of view of possible industrial electrolytic applications.

Nomenclature

| | |
|--|--|
| b | width of the inclined channel |
| D | diffusion coefficient |
| d | interelectrode distance |
| e_m | mean film thickness |
| $Gr_d = \frac{d^3 g \sin \alpha}{\nu^2}$ | Grashof number, based on d |
| $Gr_L = \frac{L^3 g \sin \alpha}{\nu^2}$ | Grashof number, based on L |
| \bar{k} | overall mass transfer coefficient, defined by Equation 9 |
| L | electrode length |
| Q_v | volumetric flow rate |
| $Q_{vl} = \frac{Q_v}{b}$ | volumetric flow rate per unit width of channel |

| | |
|-----------------------------|---|
| $Re = \frac{Q_{vl}}{\nu}$ | Reynolds number |
| $Sc = \frac{\nu}{D}$ | Schmidt number |
| $Sh_d = \frac{\bar{k}d}{D}$ | Sherwood number, based on d |
| $Sh_L = \frac{\bar{k}L}{D}$ | Sherwood number, based on L |
| $u_m = \frac{Q_{vl}}{e_m}$ | mean velocity of the liquid film |
| α | inclination angle of the channel with respect to the horizontal |
| ν | kinematic viscosity of the electrolyte |

1. Introduction

A new concept of electrochemical cell for the treatment of dilute solutions has been patented recently [1] and briefly described elsewhere [2]; the cell may be called the 'falling-film cell'. The basic idea of this cell was to transpose, from the fluid mechanics discipline, the principle of flow as a film of a liquid over a solid surface; this flow is well known in Fluid Mechanics and has received various applications in Chemical Engineering.

The principle of the cell unit is presented in

* Present address: IUT Génie Chimique, BP420, 44606, Saint Nazaire, France.

Fig. 1. The flowing inclined plane surface is one electrode, the other being a sheet of expanded metal positioned near the flowing surface so that the liquid film may be in contact with both electrodes. The cell units may be arranged in columns similar to a plate column [1].

Among the apparent advantages when compared with other new cells, there exists:

- the possibility of working with thin films of electrolyte between the electrodes and thus to treat solutions having low electrical conductivities
- the high simplicity of the overall hydrodynamics (gravity flow only) without any moving electrode

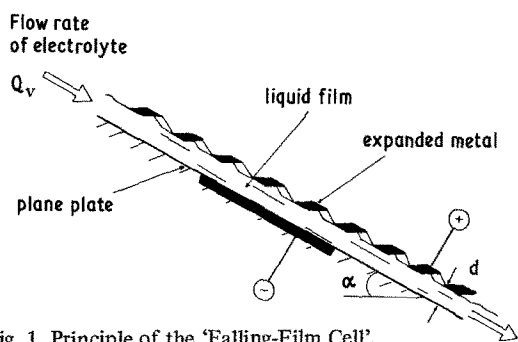


Fig. 1. Principle of the 'Falling-Film Cell'.

ease of escape of gas that may be produced at the expanded sheet of metal through the free surface of the film

The hydrodynamic aspects of the flow of thin liquid films have been intensively studied [3-6]; here, the presence of a sheet of expanded metal at the level of the film surface leads to modified hydrodynamics. It is known that a capillary effect exists near the lateral sides of a channel containing a free-falling liquid film [7] and it was hoped in the present work that such an effect could exist near every point where the free surface of the liquid enters into contact with the expanded metal. Obviously, at each of these contact points, the local velocity of the free surface is zero. The falling liquid film in the 'falling-film cell' is thus semi-confined.

The present experimental work was undertaken in order to understand the behaviour of a unit cell, with the following particular objectives:

firstly, to examine the hydrodynamic particularities of such a semi-confined film flow. Independently of the obvious application of this information in any electrolytical use of the system, it seems that such a problem has never been studied previously.

secondly, to determine the overall mass transfer coefficients at the electrodes in order to evaluate the performance of the electrochemical cell and to facilitate optimal design.

2. Experimental method

The hydrodynamic circuit is represented in Fig. 2. The liquid contained in the storage tank is pumped to a constant level reservoir from which it flows to an open box acting as the distributor of the

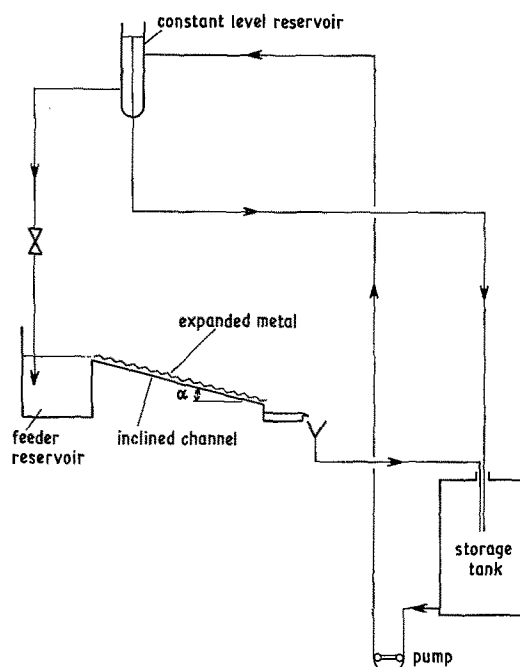


Fig. 2. Diagram of experimental flow scheme.

liquid over the inclined channel. The distributor and the channel are both 9 cm wide and are made of 'Altuglas' (a French commercial name of a material such as Plexiglas; manufactured by Altulor). Grooves in the sides (Fig. 3) allow the positioning of the sheet of expanded metal at different distances d from the bottom of the channel. The length of the inclined plate is 24 cm.

Depending on the surface (bottom of the channel or sheet of expanded metal) at which the mass transfer coefficient is measured by means of the electrochemical method, the electrodes are different:

(a) for mass transfer determination at the bottom of the channel (24 cm long; 9.3 cm wide) a rectangular surface (10 cm long; 7 cm wide) of gold and platinum plated copper is inserted in the wall. This rectangular (70 cm^2) surface acts as a cathode whereas the counter electrode (anode) is a sheet of expanded platinum plated titanium (24 cm long; 9.3 cm wide) having a total surface area of about 370 cm^2 ; this is positioned parallel to the bottom of the channel by location in the grooves mentioned previously.

(b) for mass transfer determination at the sheet of expanded metal, the whole bottom of the channel is a sheet of stainless steel and acts as the

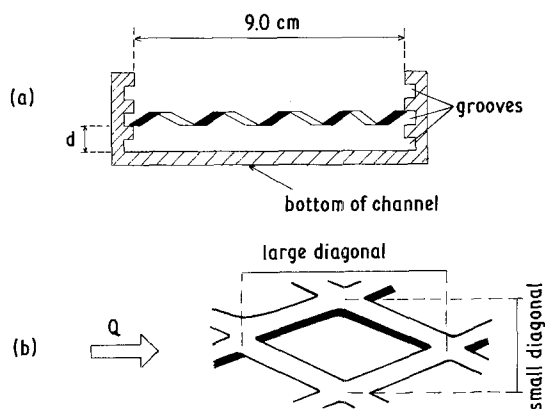


Fig. 3. Schematic representation of: (a) the setting-up of the sheet of expanded metal, (b) a mesh in a sheet of expanded metal.

anode. The sheet of expanded metal is made of copper; it is electrically insulated by painting with 'M. Coat' (protective coating manufactured by Micro-Measurements) with the exception of a rectangular surface (10 cm long; 7.1 cm wide) which is successively gold and platinum plated and constitutes the cathode.

In each case, the sheet of expanded metal is always positioned such that the larger dimension LD (see Fig. 3b) is parallel to the general flow direction of the liquid in the channel.

The mass transfer coefficients are determined by electrochemical reduction of potassium ferricyanide. The electrolyte is a mixture of $\text{Fe}(\text{CN})_6\text{K}_3$ (0.005 M) and of $\text{Fe}(\text{CN})_6\text{K}_4$ (0.05 M) in an aqueous solution (0.5 N) of sodium hydroxide. The electrolyte temperature is maintained at 20 or 30°C depending on the category of experiments (20°C for experiments (a); 30°C for experiments (b)), and nitrogen is continuously bubbled into the reservoir just upstream of the channel. At 20°C, the kinematic viscosity of the electrolyte is $\nu = 1.07 \times 10^{-2} \text{ cm}^2 \text{ s}^{-1}$ and the diffusion coefficient of the ferricyanide ions is $D = 5.63 \times 10^{-6} \text{ cm}^2 \text{ s}^{-1}$; thus the Schmidt number $Sc = \nu/D$ is 1900. At 30°C, $\nu = 0.90 \times 10^{-2} \text{ cm}^2 \text{ s}^{-1}$ and $D = 7.98 \times 10^{-6} \text{ cm}^2 \text{ s}^{-1}$; thus $Sc = 1130$.

The electrical circuit contains a Tacussel PRT 20-2 potentiostat; a Luggin capillary connected to a reference electrode (SCE) is immersed in the liquid film just down from the cathode. Polarographic curves are obtained by linear variation of

the cathode potential through a Tacussel-Servovit sweep generator and are recorded in full.

3. Mass transfer at the bottom of the channel

3.1. Experimental results

The overall mass transfer coefficient \bar{k} between the liquid film and the bottom of the channel is determined for the following ranges of variation of the parameters:

electrolyte flow rate, Q_{vl} , per unit of the channel width; $1 < Q_{vl} < 12 \text{ cm}^2 \text{ s}^{-1}$. This corresponds to a Reynolds number, $Re = Q_{vl}/\nu$ varying between 95 and 1150.

angle, α , of inclination of the channel over the horizontal; $3^\circ \leq \alpha \leq 15^\circ$

distance, d , between the bottom of the channel and the expanded sheet of metal; $1 \text{ mm} \leq d \leq 4 \text{ mm}$

The experimental variations of \bar{k} vs Q_{vl} for a given interelectrode distance, d , obey the form of the curve represented in Fig. 4a. Three zones are defined on this curve; they correspond to three different types of flow regime, which are observed during the experiments:

(a) *Zone 1*, characterized by a decrease of \bar{k} when Q_{vl} is increased is typical of the capillary flow regime. In other words, capillary phenomena exist between the free surface of the film and the sheet of expanded metal, when the mean film thickness e_m is lower than d ; menisci are formed (Fig. 4b) in the mesh of the expanded metal. The liquid flowing downwards along the bottom of the channel is forced to pass below these menisci where the flow velocity is increased; thus the mass transfer coefficient may be high at small flow rates. Figs. 5–7 show the existence of *Zone 1* on the experimental curves of \bar{k} vs Q_{vl} . As the liquid flow rate is decreased, the liquid film becomes thinner and thus the capillarity phenomenon is accentuated more; the consequence is an increase of \bar{k} when Q_{vl} diminishes. The true mean film thickness e_m is unknown and may be different from the thickness of a free-falling film, owing to the capillary effects which deform the surface of the film. However, as the formation of a meniscus is essentially initiated by the wavy state of the

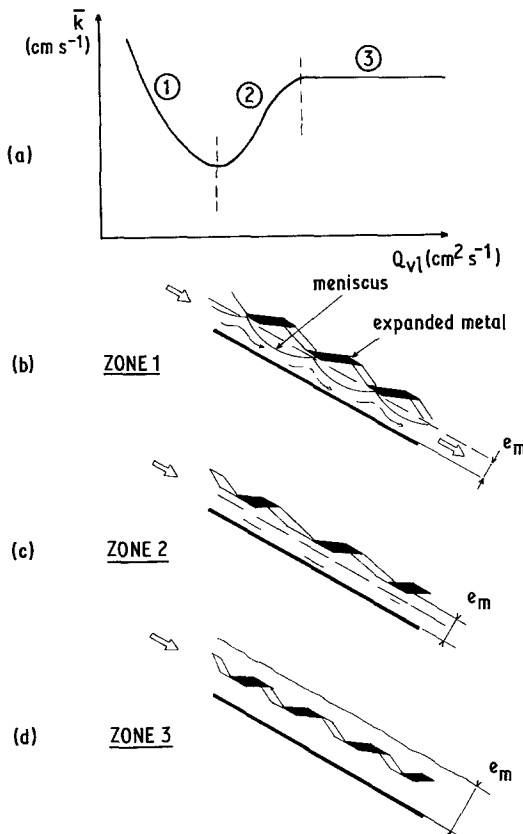


Fig. 4. Schematic representation of the different types of flow: (a) variation of \bar{k} with Q_{vl} , (b) case of the capillary flow regime, (c) case of the flow with turbulence promotion, (d) case of the existence of a flow over the expanded metal.

liquid film formed between the bottom of the channel and the expanded metal, as an approximation, e_m , could be computed from the following expression deduced by Levich [8] for the laminar wavy flow of a falling film:

$$e_m = \left(\frac{2.4\nu Q_{vl}}{g \sin \alpha} \right)^{1/3} \quad (1)$$

For a given inclination angle, α , an increase of Q_{vl} ($Q_{vl} = u_m e_m$) involves an increase of e_m and thus an increase in the mean flow velocity u_m . A decrease of \bar{k} when Q_{vl} is increased may be explained by the progressive disappearance of the meniscus and thus by the laminarization of the flow which is no longer forced to pass below these menisci.

(b) Zone 2 is characterized by an increase of \bar{k} with Q_{vl} . The end of Zone 1 corresponds to the total disappearance of the meniscus; thus the free surface of the liquid film is located within the thickness of the sheet of expanded metal which is acting as a turbulence promoter of the liquid film (Fig. 4c). Figs. 5-7 also show Zone 2 clearly.

(c) Zone 3 corresponds (Fig. 4d) to the situation where a part of the flow rate passes through and over the sheet of expanded metal; thus the fraction of the flow rate falling between the two electrodes probably remains unchanged. This may be the reason why \bar{k} is nearly constant in spite of

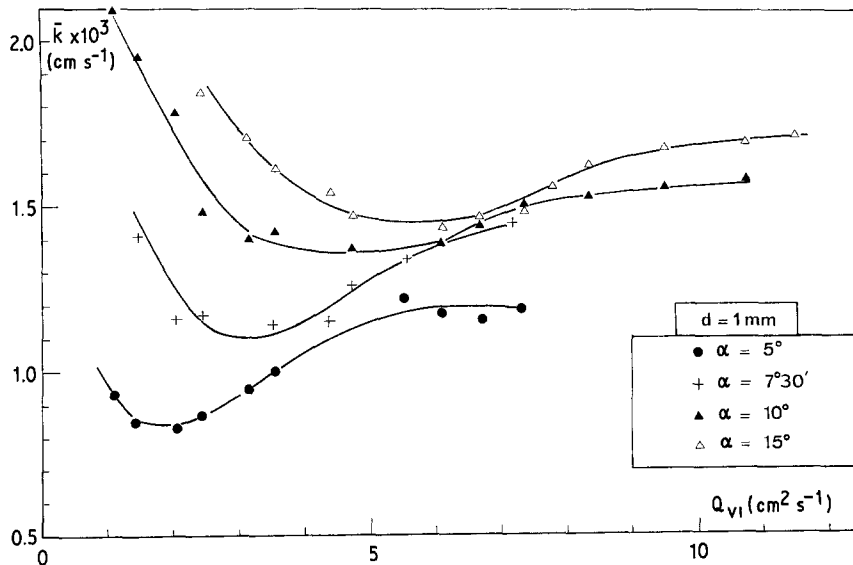


Fig. 5. Variations of \bar{k} with Q_{vl} and α , for $d = 1 \text{ mm}$.

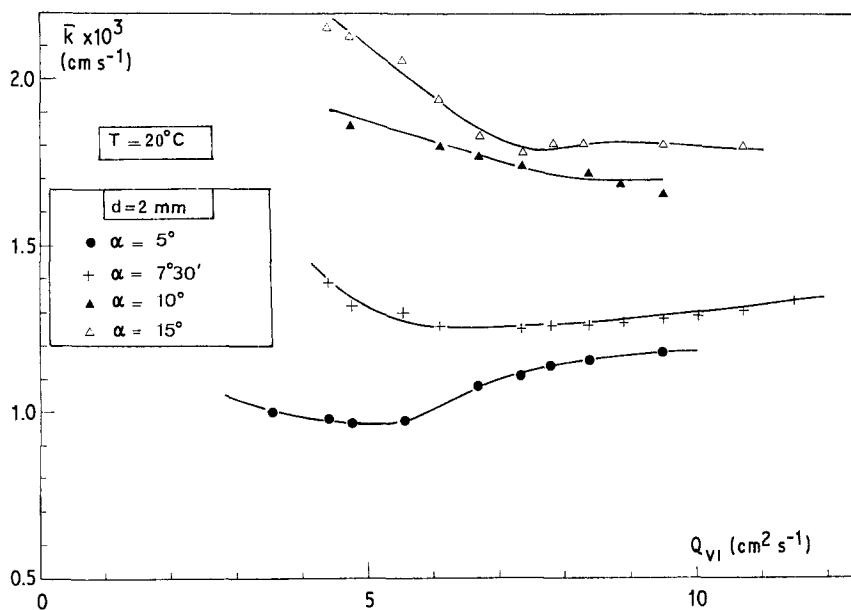


Fig. 6. Variations of \bar{k} with Q_{vl} and α , for $d = 2 \text{ mm}$.

an increase of Q_{vl} . In other words the flow rate is partially by-passed from the interelectrode space. Such situations have only been fulfilled for the smallest values of α .

Particular comments have to be made on the results of Figs. 5-7. For Zones 1 and 2, the mass transfer coefficient, \bar{k} , increases with α , when Q_{vl}

is given, independently of the value taken by the interelectrode distance d ; the same conclusion cannot be drawn for the regime of Zone 3 which is only clearly obtained in one case ($\alpha = 5^\circ$; $d = 1 \text{ mm}$), as shown in Fig. 5. Such an increase of \bar{k} when α is increased, Q_{vl} being given, is due to a decrease of the mean thickness e_m of the film and thus to an increase of u_m .

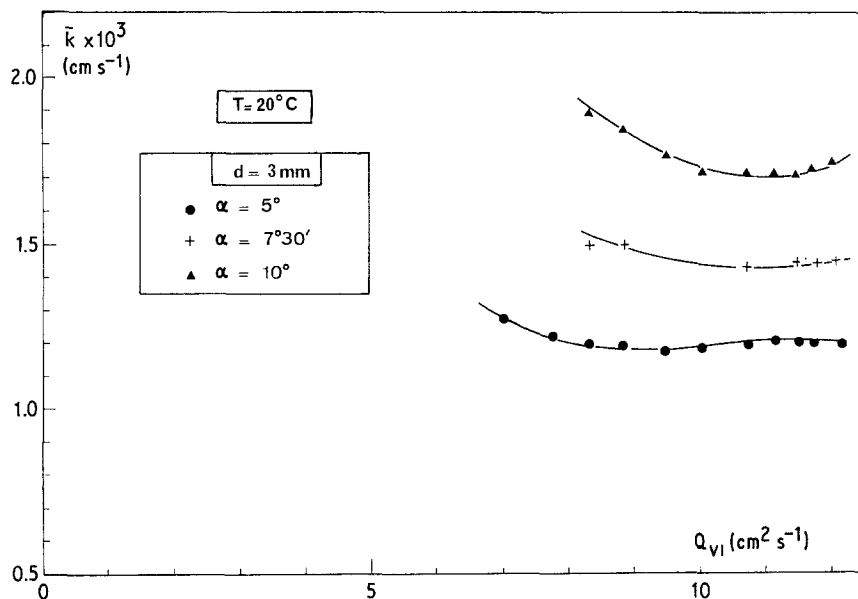


Fig. 7. Variations of \bar{k} with Q_{vl} and α , for $d = 3 \text{ mm}$.

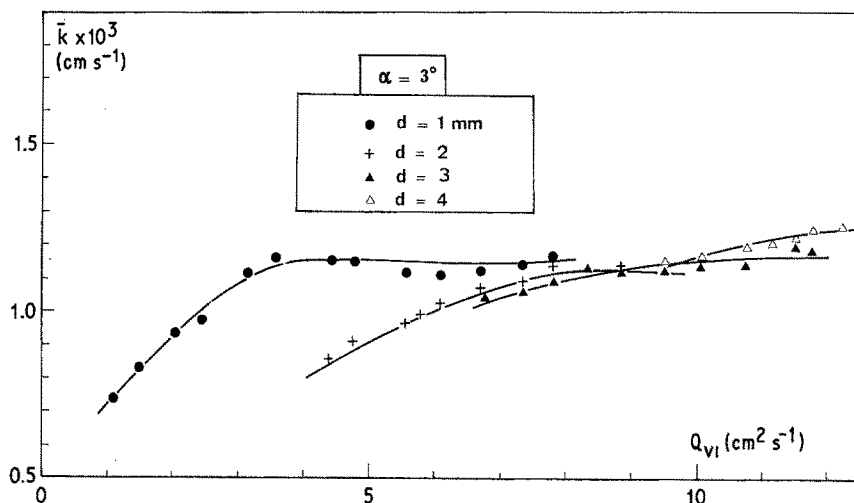


Fig. 8. Variations of \bar{k} with Q_{v1} and d , for $\alpha = 3^\circ$.

When $\alpha = 3^\circ$ (Fig. 8) the capillary regime (Zone 1) is not obtained, whatever the distance d . This may be explained by the fact that when α is lower than 5° , waves are not present at the free surface of the film or their amplitude is very small [9]. Waves appear around $Re = 1000$ – 1500 [8, 10] and one condition for the existence of the capillary regime is the existence of laminar wavy flow (the other concerning the value of d relative with e_m). Otherwise, it is difficult to analyse the

influence of d on \bar{k} owing to the fact that when α is changed, the range of variation of Q_{v1} is not the same for a given hydrodynamic flow regime. However, one notes in Fig. 9, for $\alpha = 15^\circ$, that \bar{k} increases with d .

3.2. Empirical correlations of the results

As the existence of the capillary regime depends on the relative value of d and of e_m , on the pre-

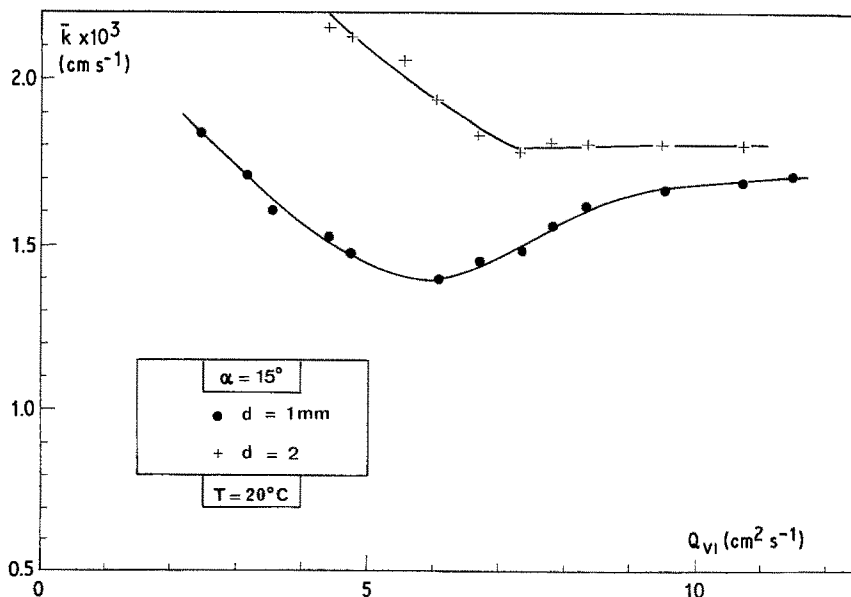


Fig. 9. Variations of \bar{k} with Q_{v1} and d , for $\alpha = 15^\circ$.

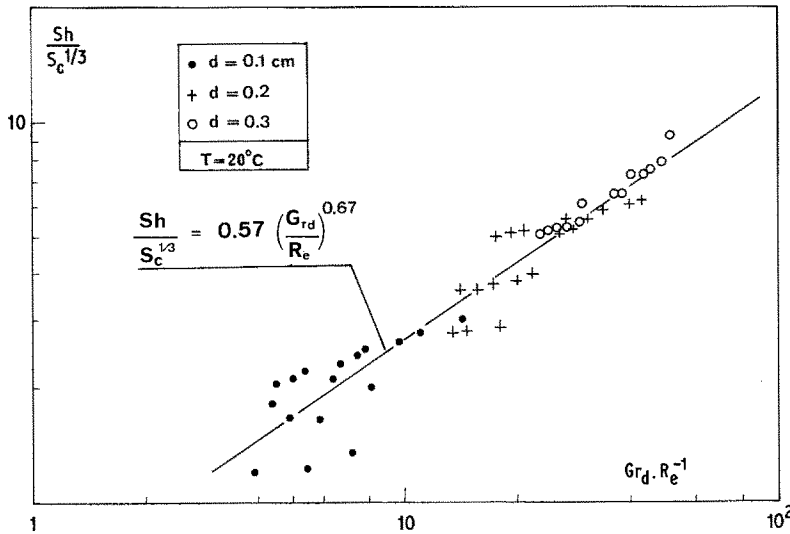


Fig. 10. Correlation for mass transfer in the capillary flow regime.

vious condition that the corresponding free film flow should be wavy, the ratio $d:e_m$ is chosen as the determining parameter. Otherwise, as e_m is unknown for this capillary flow regime, it is supposed that Equation 1 may be applied in the following form:

$$e_m = K \left(\frac{\nu Q_{v1}}{g \sin \alpha} \right)^{1/3} \quad (2)$$

where K is an arbitrary constant including the effect of the presence of the expanded metal. Thus:

$$\frac{d}{e_m} = \frac{d}{K} \left(\frac{g \sin \alpha}{\nu Q_{v1}} \right)^{1/3} \quad (3)$$

or

$$\left(\frac{d}{e_m} \right)^3 = \frac{1}{K} Gr_d Re^{-1} \quad (4)$$

where $Gr_d = d^3 g \sin \alpha / \nu^2$ is the Grashof number defined relative to d as the characteristic dimension.

The deduction of the empirical correlation is made by regressive analysis by assuming that Sh is proportional to $Sc^{1/3}$, as shown in the correlation describing mass transfer for a free-falling film [10].

(a) For the capillary flow regime, the empirical correlation obtained with a correlation coefficient of 0.96 is the following:

$$Sh_d = \frac{\bar{k}d}{D} = 0.57 Sc^{1/3} \left(\frac{Gr_d}{Re} \right)^{0.67} \quad (5)$$

The expression shows that \bar{k} decreases when Q_{v1}

(or Re) and α (or Gr_d) are separately increased. It is compared in Fig. 10 with the experimental results. The correlation of Equation 5 is valid only when $Re < Re_c$ where Re_c represents a critical Reynolds number between Zones 1 and 2. The value Re_c of Re corresponds to the value of Q_{v1} which leads to the minimum value of \bar{k} between Zones 1 and 2 (Figs. 5-7). Re_c depends on d and on α , which leads to an expression for Re_c as a function of Gr_d ; it follows then (Fig. 11) that:

$$Re_c = 24.5 Gr_d^{0.36} \quad (6)$$

(b) For the flow regime corresponding to Zone 2 where the expanded metal acts as a turbulence promoter, the correlation of the results has to account for an increase of \bar{k} with both parameters Q_{v1} and α . It is found (correlation coefficient of 0.98) that:

$$Sh_d = 0.035 Sc^{1/3} (Re Gr_d)^{0.30} \quad (7)$$

and this equation is compared in Fig. 12 with the experimental results. Let us recall that for a free-falling liquid film in the laminar wavy regime, the mass transfer to the bottom of the channel was correlated (correlation coefficient of 0.97) as:

$$Sh_L = \frac{\bar{k}L}{D} = 1.0 Sc^{1/3} Gr_L^{2/9} Re^{1/9} \quad (8)$$

L being the length of the transfer surface in the flow direction [10]. In Equation 7 the influence of Q_{v1} and of α is more important than in Equation 8, which may express the turbulence promoting effect of the expanded metal.

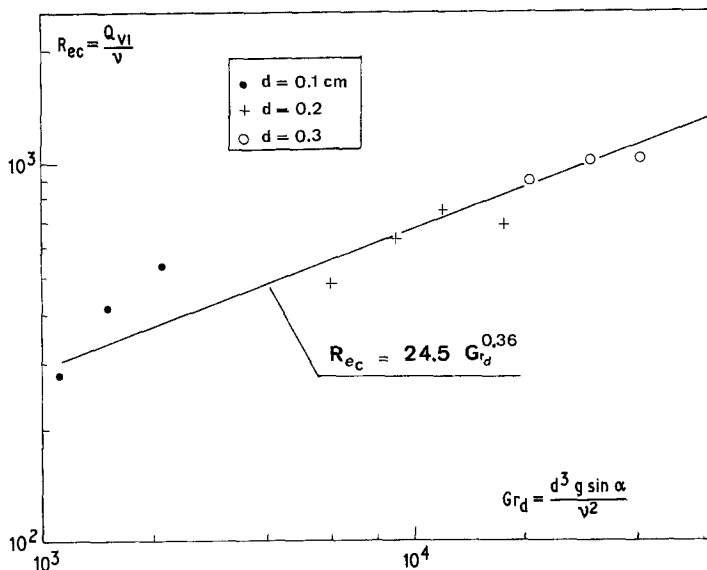


Fig. 11. Stability curve of the capillary flow regime: $Re_c = f(Gr_d)$.

Concerning the third flow regime (Zone 3) no correlation was attempted because only a few results were obtained in Zone 3 and also because the corresponding flow is not interesting from the electrochemical engineering point of view.

4. Mass transfer at the expanded metal

As the fractional surface area, A , of the expanded metal which is immersed within the electrolyte is unknown and varies with the hydrodynamic conditions, the calculation of the mass transfer coefficient, \bar{k} , from the limiting current I_L is

impossible. Only the product $\bar{k}A$ can be determined from I_L through the expression:

$$\bar{k}A = \frac{I_L}{zFC_s} \tag{9}$$

which is currently used for the deduction of mass transfer coefficients. In Equation 9, C_s is the ferricyanide concentration, F the Faraday number and z the number of electrons in the reaction ($z = 1$). The flow rate Q_{v1} per unit width of the channel is varied between 1.25 and 2.50 $\text{cm}^2 \text{s}^{-1}$; d is maintained constant and equal to 0.1 cm, whereas α is varied between 5 and 15°.

Fig. 13 presents the values of $\bar{k}A$ as function of Q_{v1} for various angles α , but the influence of the latter cannot be shown because the effective electrode area A (and thus $\bar{k}A$) also depends on α . When α is given, $\bar{k}A$ increases with Q_{v1} . Such an increase is due to two inter-dependent phenomena: on one hand the increase of the electrode area A with Q_{v1} , on the other hand the increase of the percentage of obstacles acting as turbulence promoters.

5. Comparison and discussion

Fig. 13 reports experimental values of $\bar{k}A$ corresponding to mass transfer determinations at the bottom of the channel (rectangular electrode area with $A = 70 \text{ cm}^2$) under the same flow rate and temperature conditions as for mass transfer exper-

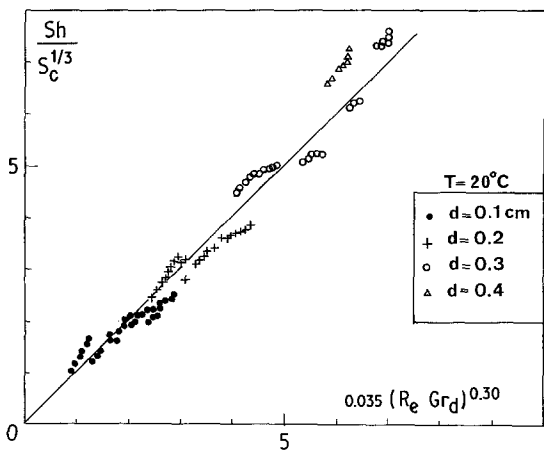


Fig. 12. Correlation for mass transfer in the flow regime with turbulence promotion.

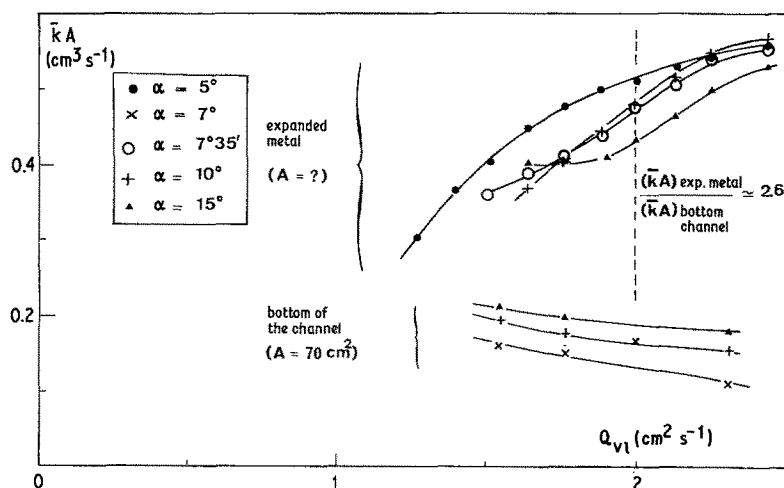


Fig. 13. Comparison between mass transfer results at the bottom of the channel and at the sheet of expanded metal.

iments at the expanded metal; d is 0.1 cm. The decrease of $\bar{k}A$ when Q_{vl} is increased, is typical of the existence of a capillary flow.

The comparison between both categories of results is made difficult by the fact that the active fractional area of the expanded metal is unknown. Let us consider that the total area $A = 107 \text{ cm}^2$ of the electrode of expanded metal is active; thus the ratio of this area to the rectangular electrode area of 70 cm^2 is 1.53. When compared with the ratio of the $\bar{k}A$ values at both mass transfer surfaces which, for example, at $Q_{vl} = 2 \text{ cm}^2 \text{ s}^{-1}$ is around 2.6 (see Fig. 13), one concludes that \bar{k} at the expanded metal is higher than \bar{k} at the bottom of the channel.

A higher diffusional mass transfer to the sheet of expanded metal is probably due to the capillary phenomenon which is known to modify the local velocities near the surfaces on which menisci are formed [7]. Indeed, for free-falling liquid film flow in an inclined channel, it has been shown that the liquid flow velocity is maximum near the lateral sides of the channel where a capillary effect is present and leads to local film thicknesses which are higher than in the middle of the channel [7]. From Equation 1, and owing to the fact that $Q_{vl} = u_m e_m$, one deduces that the liquid velocity is a growing function of the film thickness; this may explain why higher velocities exist near the expanded metal.

Also, there is similarity with electrochemical mass transfer to the walls of pores in fuel cells where menisci are formed. It has been shown that the presence of capillary phenomena over one elec-

trode is responsible for micro-convection effects below the meniscus thus leading to higher mass transfer coefficients at that electrode [11].

An important aspect of the present experimental work is the evidence for the existence of a flow regime for which a capillary effect is located at the expanded metal; the domain of existence of this regime depends on the inclination angle α and on the interelectrode distance d . When it exists, the capillary flow regime allows high mass transfer coefficients \bar{k} at low flow rates Q_{vl} in contrast with classical electrochemical systems with forced flow. One knows that the space-time yield of an electrochemical cell is increased by increasing the ratio $\bar{k} : Q$ and that more or less sophisticated means are proposed (rotating cylinder or disc electrodes, for example) [12]. Here, a simple gravity flow without any moving parts leads to \bar{k}/Q values which are higher when Q is decreased, thus allowing relatively high conversions per pass at small flow rates.

Another advantage follows from the thinness of the liquid film, i.e. of the possible interelectrode distance d . Ideally, values of d around 0.1 cm seem to be indicated, thus allowing the application of the system to the electrolytic treatment of low conductivity solutions. A further paper will report the application to copper recovery from very dilute solutions [13].

In this capillary flow regime, the presence of menisci all along the length and the width of the inclined plate leads to a pseudo-uniformity of the distribution of the local mass transfer coefficients, a situation which may be useful for the scale-up

of the cell. The volume element corresponding to a meniscus may be considered as a unit hydrodynamic element of the system.

The value of the inclination angle α determines the existence of the capillary flow regime. Indeed, α has to be sufficiently high for the liquid film to be wavy enough for formation of the meniscus to occur.

6. Conclusions

A new type of electrochemical cell uses the gravity flow of electrolyte over an inclined plate and below a sheet of expanded metal positioned above and parallel to the plate. Mass transfer determinations at the electrodes of such a cell have shown the existence of three distinct flow regimes. Two of these regimes (capillary flow and turbulence promotion flow) may be used in the application of the cell, the best being probably the capillary flow regime since the mass transfer coefficient is high at low flow rates. Empirical correlations have been proposed for mass transfer at the plane plate in both regimes.

References

- [1] F. Coeuret and J. Legrand, French Patent No. 81 19115 (1981).
- [2] J. Legrand and F. Coeuret, 34th I.S.E. Meeting, Extended Abstract 0402, Erlangen, R.F.A. (1983).
- [3] G. D. Fulford, *Adv. Chem. Eng.* **5** (1964) 151.
- [4] A. Iribarne, A. D. Gosman and D. B. Spalding, *Int. J. Heat Mass Transfer* **10** (1967) 1661.
- [5] A. A. Wragg, P. Serafimidis and A. Einarsson, *ibid.* **11** (1968) 1287.
- [6] A. A. Wragg and A. Einarsson, *Chem. Eng. Sci.* **25** (1970) 67.
- [7] A. M. Binnie, *J. Fluid Mech.* **5** (1959) 561.
- [8] V. G. Levich, 'Physicochemical Hydrodynamics', (Prentice Hall, Englewood Cliffs, New Jersey, (1962).
- [9] D. Campergue, Thesis, Université de Poitiers, France (1973).
- [10] J. Legrand and F. Coeuret, submitted for publication.
- [11] F. G. Witt, *J. Electrochem. Soc.* **110** (1963) 145.
- [12] F. Coeuret and A. Storck, *Informations Chimie (France)* **210** (1981) 121.
- [13] F. Coeuret and J. Legrand, to be submitted.